Dual-Band Multi-Receiver Wireless Power Transfer with Reactance Steering Network

Ming Liu, *Member, IEEE,* Minjie Chen, *Member, IEEE*
Department of Electrical Engineering
Andlinger Center for Energy and the Environment
Princeton University, Princeton, NJ, USA
Email: ml45@princeton.edu, minjie@princeton.edu

***Abstract*—Wireless power transfer (WPT) via near-field magnetic coupling is an enabling technology for many applications including consumer electronics and electric vehicles. A few WPT standards have been established with frequencies ranging from kHz to MHz. MHz operation offers smaller size and higher tolerance to coil misalignment, and kHz operation offers higher efficiency and higher power rating. This paper presents a dual-band multi-receiver (DBMR) WPT architecture targeting applications with very wide load impedance variation. The key innovation is a novel reactance steering network (RSN) that can seamlessly compensate an arbitrary load impedance for radio-frequency (RF) power amplifiers. The proposed approach is generally applicable to a variety of high-frequency power conversion applications. A dual-band reconfiguable WPT system that can efficiently power multiple 100 kHz and 13.56 MHz receivers across a very wide misalignment range is built and tested to validate the proposed RSN technique.**

***Index Terms*—wireless power transfer, reactance steering network, high frequency power conversion.**

I. Introduction

Wireless power transfer (WPT) through near-field magnetic coupling is an enabling technology for many applications ranging from consumer electronics to electric vehicles [1]–[3]. A few WPT standards have been established (e.g., AirFuel, Qi) with frequencies ranging from hundreds of kHz to a few MHz. These standards may merge and may cover many frequency domains in the future. In general, there is a fundamental tradeoff between kHz operation and MHz operation in WPT: MHz operation enables long distance power transfer and better robustness against coil misalignment, while kHz operation offers higher efficiency and higher power transfer capability. Both kHz and MHz WPT standards will co-exist for a long period of time for different application scenarios.

Figure 1 illustrates an application scenario where a dual-band transmitter is loaded with multiple receivers. The dual-band transmitter simultaneously charges a cellphone at 13.56 MHz and charges a laptop and a LED lamp at 100 kHz. The transmitting coils and the receiving coils may be loosely coupled or closely coupled. The load impedance on the transmitter side may change across a wide range. The transmitter needs to maintain high performance at both kHz and MHz, and the receiver should achieve high efficiency and maintain low EMI. Circuits that can enable dual-band multi-receiver wireless power transfer with high robustness against coil misalignment are needed and are the main focuses of this paper.

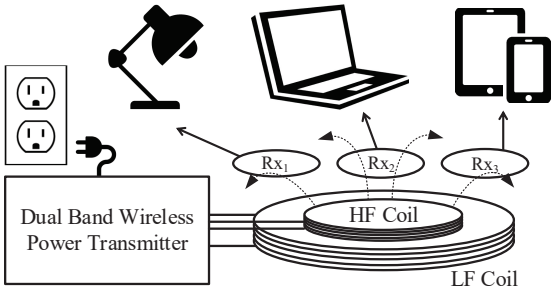

Fig. 1. Application scenario of a dual-band multi-receiver WPT system. The dual-band transmitter drives multiple receivers at two different frequencies.

Maintaining resistive load for high-frequency inverters (e.g., Class-E [5]) is critical in achieving high efficiency and high power transfer capability. There exist many design techniques that can compress load resistance variation for single switch inverters [6]–[9]. However, for reactance variation, the most common solution is to use a separate tunable matching network (TMN) [10]. These additional passive components and switching devices increase the volume, reduce the efficiency and increase the cost. Moreover, the resolution of these compensation methods depends on the number of components used in the matching network. Precise and seamless reactance compensation is not achievable with the TMN technique, especially with significant reactance variation.

This paper presents a dual-band multi-receiver (DBMR) WPT architecture based on a reactance steering network (RSN) that can maintain high performance across very wide misalignment range for WPT. It comprises a low-frequency (LF) transmitter and a high-frequency (HF) transmitter. Instead of designing two single-frequency transmitters and operating them together, developing a dual-band reconfiguable system can create mutual advantages to improve the performance, shrink the size and reduce the cost. The key principle of the RSN technique is to split the power flow in a two-branch L-C network to compensate the load reactance variation seen by the HF transmitter. With strategic amplitude and phase modulation, the load impedance of the two HF inverters can be maintained pure resistive across a very wide load impedance range. Compared to the TMN techniques, this solution significantly reduces the components counts and improves the efficiency. Moreover, by using the RSN technique, the WPT

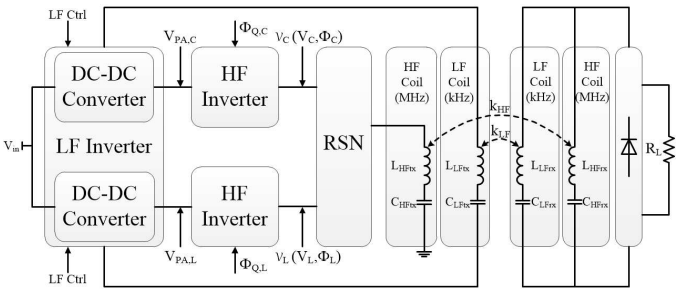

Fig. 2. Block diagram of the dual-band multi-receiver WPT architecture.

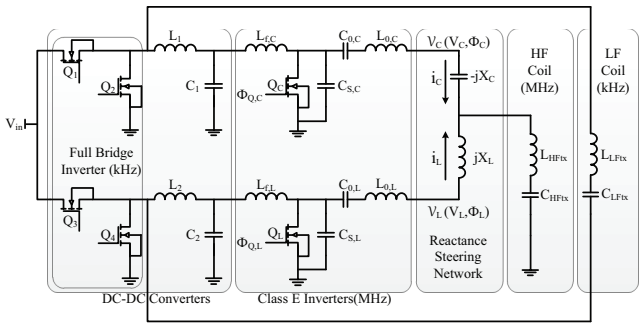

Fig. 3. Schematic of an example DBMR system comprising a RSN, two Class-E PAs, two buck converters and two transmitting coils.

system operates much more robust against coil misalignment. The RSN technique and design methods are applicable to a wide range of high frequency power electronics applications.

II. Dual-Band Multi-Receiver WPT with RSN

Figure 2 shows the block diagram of the proposed dual-band multi-receiver (DBMR) WPT architecture with the reactance steering network (RSN). The transmitter side comprises two LF dc-dc converters operating at 100 kHz, two HF inverters operating at 13.56 MHz, a reactance steering network (RSN), a LF transmitting coil, and a HF transmitting coil. The receiver side comprises a dual-band receiver and multiple single-band rectifiers. The two dc-dc converters modulate the inputs of the HF inverters, and simultaneously drive the LF transmitting coil. By modulating the voltage amplitude and the phase of the two HF inverters following a "reactance-steering" approach, the two HF inverters see pure resistive load. The dc-dc converters also drive the LF transmitting coil as a phase-shift full bridge, transferring power at both LF and HF simultaneously.

Each of the function block in the proposed architecture can be implemented in multiple ways: the LF inverters can be implemented as Class-D or full-bridge inverters; the low-pass filters at the output of the LF inverters can be implemented as L-networks or π-networks; the HF inverters can be implemented as Class-E, Class-F or Class-Φ inverters; the RSN can be implemented as a three-port LC network or other three-port network types. The LF and HF transmitting coils are standard transmitting coils tuned for nominal coupling coefficients. The dc-dc converters drive the LF coil, and the HF inverters drive the HF coil. The key attributes of this architecture are: 1) the LF inverters and the low-pass filters function as dc-dc converters with adjustable output voltages; 2) the two HF

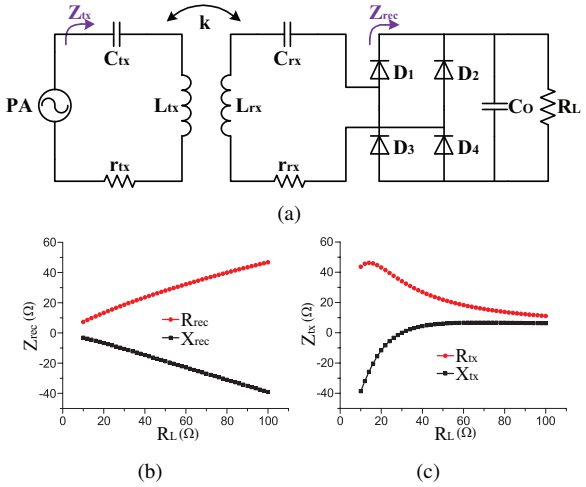

Fig. 4. Circuit model and simulated rectifier impedance (Z_{rec}) and transmitter coil input impedance (Z_{tx}) as the load resistance (R_L) change in an example MHz WPT system considering device parasitics.

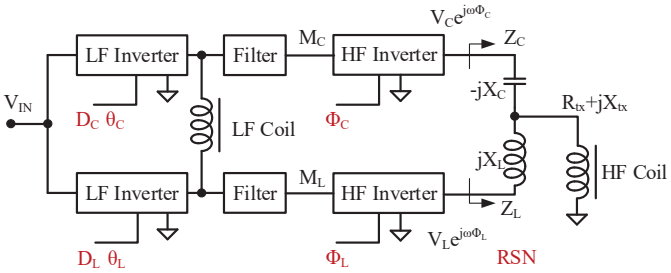

Fig. 5. Simplified block diagram of the RSN architecture. This architecture has six input variables: D_C, D_L, θ_C, θ_L, Φ_C, Φ_L, and independently drives the LF coil and the HF coil.

inverters are precisely phase-shifted against each other; 3) the element values of the RSN are strategically selected to cover the targeted load impedance range.

Fig. 3 shows the schematic of an example implementation of the RSN architecture with half-bridge LF inverters, LC low pass filters, and Class-E HF inverters. The two half-bridge inverters and the low-pass filters function as two buck converters that modulate the inputs of the two Class-E inverters. The two Class-E inverters are loaded by a LC resonant network including an inductive branch jX_L and a capacitive branch $-jX_C$. This circuit should be controlled following a "reactance steering" approach to maintain pure resistive load at both the HF inverters.

III. Reactance Steering Network for HF WPT

The transmitter coil impedance (Z_{tx}) and the rectifier impedance (Z_{rx}) of a typical MHz WPT system as shown in Fig. 4(a) can change across a wide range as the load impedance (R_L) and the coupling coefficient (k) change. Fig. 4(b)-(c) plots the Z_{tx} and Z_{rx} as functions of R_L in an example circuit considering device parasitics. As illustrates, the impedance variation detunes the resonance of the transmitter coil and degrades the performance of the RF-inverter. Here we introduce a "reactance steering" approach for the RSN architecture to maintain high performance against the impedance variation.

A simplified block diagram of the RSN architecture is shown in Fig. 5. The key element of the RSN architecture is the three port network comprising jX_L and $-jX_C$. Different from the *RCN* [6], [7] or the *Outphasing* [8] concepts, where X_L equals X_C, here X_L and X_C can be different can be optimally chosen based on the load impedance range. The input impedance of the transmitter coil is (Z_{tx} = R_{tx} + jX_{tx}). The phase and amplitude of the output of the two HF inverters ($V_C e^{j\omega\Phi_C}$, $V_L e^{j\omega\Phi_L}$), can be controlled independently, thus:

- if Z_{tx} is resistive, the two HF inverters equally share power and both see pure resistive load;
- if Z_{tx} is inductive, the system steers power towards the capacitive branch. The capacitive element $-jX_C$ is used to compensate the inductive Z_{tx};
- if Z_{tx} is capacitive, the system steers power towards the inductive branch. The inductive element jX_L is used to compensate the capacitive Z_{tx};
- by adjusting the ratio between V_L and V_C, and the phase difference between Φ_L and Φ_C, the reactance used for compensation at each branch can be precisely controlled to maintain resistive load for both HF inverters.

The reactance steering network can be implemented in many different ways for many different applications beyond wireless power transfer. Generally speaking, by adjusting the voltage amplitude and phase shift between the two HF inverters, the system steers power towards the inductive branch or capacitive branch to seamlessly compensate the changing reflected reactance looking into the HF transmitter.

A. Voltage Amplitude and Phase Shift of the RSN

This architecture has six control inputs: D_C and D_L are the duty ratios of the two dc-dc converters; θ_C and θ_L are the phases of the two dc-dc converters; Φ_C and Φ_L are the phases of the two HF inverters. The two intermediate dc voltages M_C and M_L are controlled by D_C and D_L. To simplify the analysis, we assume $X_C = X_L = X_O$ and model the two HF inverters as two ac voltage sources: $V_C^* = V_C e^{j\Phi_C}$ and $V_L^* = V_C e^{j\Phi_L}$. The amplitudes (V_L, V_C) and phases (Φ_L, Φ_C) can be independently selected. A RSN with equal X_C and X_L can symmetrically compensate an inductive or capacitive load. Applying superposition rules, the effective load impedance of the two inverters, Z_C and Z_L, are explicit functions of X_O, R_{tx}, X_{tx} and K_{LC}^*:

$$Z_C = \frac{X_O^2}{R_{tx} - K_{LC}^* R_{tx} + (X_{tx} + X_O - K_{LC}^* X_{tx})j}, \quad (1)$$

$$Z_L = \frac{X_O^2}{R_{tx} - \frac{1}{K_{LC}^*} R_{tx} + (X_{tx} - X_O - \frac{1}{K_{LC}^*} X_{tx})j}. \quad (2)$$

Here K_{LC}^* is the complex voltage ratio between the inductive branch and capacitive branch: $K_{LC}^* = \frac{V_L}{V_C} e^{j(\Phi_L - \Phi_C)}$. Set both Z_C and Z_L as pure resistive, we get:

$$\begin{aligned} \frac{V_L}{V_C} &= \frac{X_{tx}\cos(\Delta_{LC}) - R_{tx}\sin(\Delta_{LC})}{X_{tx} - X_O} \\ &= \frac{X_{tx} + X_O}{X_{tx}\cos(\Delta_{LC}) + R_{tx}\sin(\Delta_{LC})}. \end{aligned} \quad (3)$$

$$\sin^2\Delta_{LC} = \frac{X_O^2}{X_{tx}^2 + R_{tx}^2}. \quad (4)$$

Here $\Delta_{LC} = \Phi_L - \Phi_C$ is the phase difference between the two HF inverters. For a load impedance range $R_{tx} \in [R_{min}, R_{max}]$, $X_{tx} \in [X_{min}, X_{max}]$, to ensure a solution for Δ_{LC}, X_O should be selected such that $X_O^2 \leq (X_{tx}^2 + R_{tx}^2)$ holds true across the entire R_{tx} and X_{tx} range. If $X_{max} > R_{min}$, X_O should be selected as R_{min}. Note the range of $|K_{LC}|$ guides the design of the dc-dc converters. $|K_{LC}|$ reaches maximum when $X_{tx} = X_O$ and $R_{tx} = R_{min}$, $\max(|K_{LC}|) = \sqrt{2}$. $|K_{LC}|$ reaches minimum when $X_{tx} = -X_O$ and $R_{tx} = -R_{min}$, $\min(|K_{LC}|) = 1/\sqrt{2}$. As a result, a $|K_{LC}|$ range between $\frac{1}{\sqrt{2}}$ and $\sqrt{2}$, and a Δ_{LC} range between $0°$ and $90°$ can cover an arbitrary load impedance range.

For each pair of R_{tx} and X_{tx}, there are four feasible solutions for K_{LC}^*, one located in each quadrant. Due to phase and polarity symmetry, the solution in the 1^{st} quadrant is equivalent to the solution in the 3^{rd} quadrant; and the solution for the 2^{nd} quadrant is equivalent to the solution in the 4^{th} quadrant. A first quadrant solution of K_{LC}^* is usually preferable because keeping Δ_{LC} close to zero can minimize the converter stress. In the first quadrant:

$$K_{LC} = |\frac{V_L}{V_C}| = \frac{X_O + X_{tx}}{X_{tx}\cos(\Delta_{LC}) + R_{tx}\sin(\Delta_{LC})} \quad (5)$$

$$\Delta_{LC} = \Phi_L - \Phi_C = \arcsin\sqrt{\frac{X_O^2}{X_{tx}^2 + R_{tx}^2}} \quad (6)$$

For a typical voltage source inverter, V_L is linearly proportional to M_L and D_L, and V_C is linearly proportional to M_C and D_C. As a result, the ZVS of both HF inverters can be controlled by modulating D_C, D_L, Φ_C and Φ_L, respectively. Eq. (5) and (6) are sets the control guidelines for D_L, D_C, Φ_L, Φ_C. As long as Eq. (5) and (6) hold, the load impedance of the two HF inverters are pure resistive.

Note if the load reactance is higher than the reactance of the RSN, i.e., $X_{tx} \notin [-X_C, X_L]$, the voltage amplitude ratio and phase-shift determined by Eq. (5) and (6) result in a negative resistance on one branch of the inverter, indicating that a portion of the power circulates between the two inverter branches. One branch of the inverter function as a rectifier and recycles a portion of the energy back to the source. In other words, with very high target reactance, the RSN architecture uses switched-mode power converters to synthesize an effective reactance and creates a high-Q loop to compensate the load reactance.

In summary, the principle of designing a RSN architecture is to select an optimal X_O, and control D_L, D_C, Φ_L, Φ_C based on R_{tx} and X_{tx}. A small X_O guarantees $X_O^2 \leq (X_{tx}^2 + R_{tx}^2)$, yield pure resistive load on both branches, at the cost of high circulating current when $|X_{tx}| > |X_O|$. A large X_O eliminates the circulating current when $|X_{tx}| > |X_O|$. However, for some R_{tx} and X_{tx} values, there is no solution for Δ_{LC}, and the inverters will not see pure resistive load. One needs to make tradeoffs between conduction loss (circulating current) and switching loss (lost ZVS) to optimize the system performance.

If the reactance variation is asymmetric, i.e. the reactance range is either more inductive or more capacitive, one could

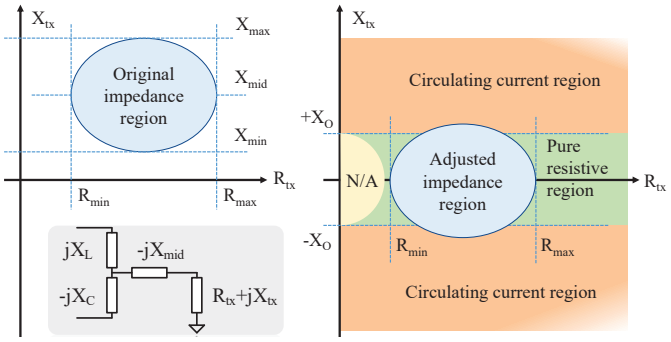

Fig. 6. (a) Targeted impedance compensation range; (b) lumped circuit model; (c) impedance compensation region for a specific choice of X_O.

add an additional impedance network in series with the load (i.e., the transmitting coil) to make the reactance range symmetric, then apply the previously described design method.

B. Design Guideline for the RSN Architecture

As illustrated in Fig. 6, for an arbitrary load impedance $R_{tx} \in [R_{min}, R_{max}]$, $X_{tx} \in [X_{min}, X_{max}]$, one can add a series impedance $-X_{mid}$ to move the original impedance region to an adjusted impedance region, which is symmetric in reactance (half-inductive, half-capacitive). If $R_{min} > \frac{X_{max}-X_{min}}{2}$, a $X_O \in [\frac{X_{max}-X_{min}}{2}, R_{min}]$ will enable pure resistive load for the entire load impedance range. If $R_{min} < \frac{X_{max}-X_{min}}{2}$, there are two options for X_O:

1) $X_O < R_{min}$: this selection of X_O enables impedance compensation for $R_{tx} \in [R_{min}, R_{max}]$ and $X_{tx} \in [-R_{min} + X_{min}, R_{min} + X_{min}]$. If $X_{tx} \notin [-R_{min} + X_{min}, R_{min} + X_{min}]$, the two HF inverters still see resistive load, but one of the inverter function as rectifier and circulates current.

2) $X_O > \frac{X_{max}-X_{min}}{2}$: this selection of X_O enables impedance compensation for $(X_{tx}^2 + R_{tx}^2) \geq X_O^2$. If $(X_{tx}^2 + R_{tx}^2) \leq X_O^2$, the HF inverters will not see pure resistive load, but the effective reactance at the inverters can be significantly reduced. ZVS may not be achievable. No inverter functions as a rectifier and there is no circulating current.

C. Design Example and Analysis

We present the design of an RSN architecture in detail through an example: R_{tx} varies from 1Ω to 5Ω; X_{tx} varies from $-2j\Omega$ to $2j\Omega$; and X_O is selected as $1j\Omega$. Based on KCL and KVL, we calculate the effective resistance seen at the inductive branch (R_L) and capacitive branch (R_C), respectively, to analyze the power flow. Fig. 7(a)-(d) show the calculated K_{LC}, Δ_{LC}, R_L and R_C as functions of R_{ts} and X_{ts}. These graphs can be used to set up the control strategy for the low frequency inverters as the load reactance changes. As previously derived, a voltage amplitude ratio adjustable from $1/\sqrt{2}$ to $\sqrt{2}$, and a phase shift adjustable from $0°$ to $90°$ can cover an arbitrary load impedance range.

As shown in Fig. 7, with an inductive load ($X_{tx} > 0$), V_C should be smaller than V_L to deliver more power through the capacitive branch; with a capacitive load ($X_{tx} < 0$), V_L should be smaller than V_C to deliver more power through the

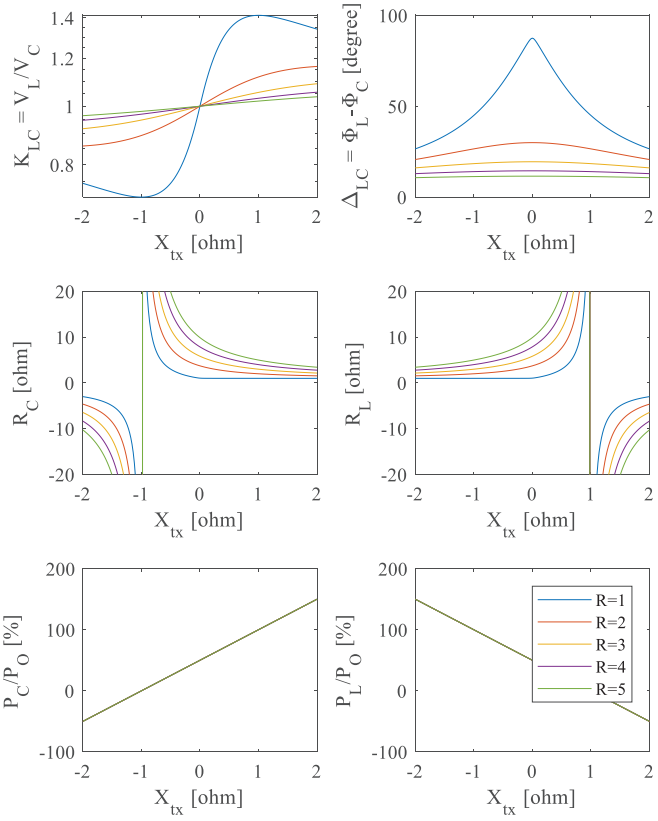

Fig. 7. (a) V_L/V_C; (b) Δ_{LC}; (c) resistance of the capacitive branch; (d) resistance of the inductive branch; (e) percentage of the power on the capacitive branch; (f) percentage of the power on inductive branch. P_C: power of capacitive branch; P_L: power of the inductive branch; P_O: output power.

inductive branch. When $|X_{tx}| \leq |X_O|$, both R_L and R_C are higher than the overall load resistance, indicating that the two inverters are sharing power. When $|X_{tx}| > |X_O|$ (i.e., the load reactance is very high), one of R_L and R_C is smaller than the overall load resistance, and the other one is negative, indicating that there exists circulating power between the two branches. One inverter branch functions as a rectifier.

Fig. 7(e)-(f) shows the power sharing percentage between the inductive and capacitive branch for this example RSN design. As expected, with pure resistive loads (i.e., $X_{tx} = 0$), the two branches evenly share power (50% each branch); with capacitive loads ($X_{tx} < 0$), the inductive branch delivers more power; with inductive loads ($X_{tx} > 0$), the capacitive branch delivers more power; with very high capacitive loads ($X_{tx} < -X_O$), power circulates from the inductive branch to the capacitive branch; with very high inductive loads ($X_{tx} > X_O$), power circulates from the capacitive branch to the inductive branch. If circulating current exists, one inverter function as a rectifier with pure resistive input impedance. Compared to a conventional tunable matching network with discrete compensation elements, the proposed RSN architecture has the following advantages:

- It can seamlessly compensate an arbitrary load impedance range and maintain pure resistive load;
- It requires very few additional component compared to a conventional TMN approach;

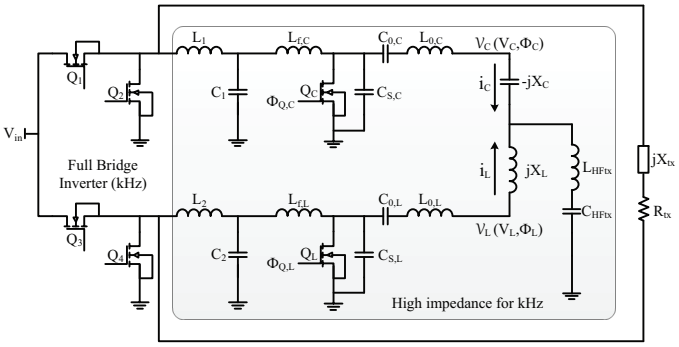

Fig. 8. Schematic of the DBMR WPT system with a phase-shift full bridge low frequency transmitter, and a RSN-based high frequency transmitter.

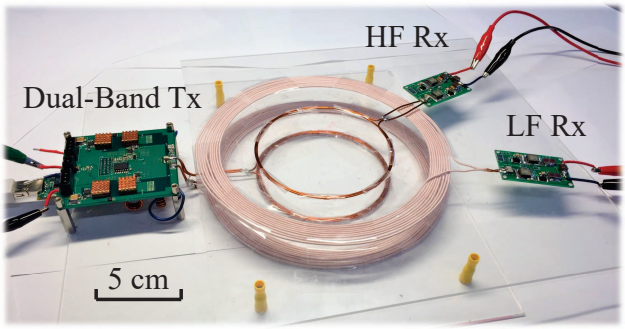

Fig. 9. The prototype DBMR WPT system with a dual-band transmitter, a pair of HF coils, a pair of LF coils, and two receivers.

- It has smooth transient behavior without mode-switching spikes or harmonics;
- The dc-dc converters in the RSN architecture can be used to drive a LF transmitter with no additional components.

IV. Low Frequency Operation of the DBMR System

One way to implement the two dc-dc converters is to build them as two buck converters with two half-bridge inverters. The two half-bridge inverters can drive a LF coil as a phase-shift full bridge, while at the same time modulate the dc voltages M_C and M_L for the HF inverters. The LF power transfer is controlled by the phase of the two LF inverters θ_L and θ_C. The output M_L and M_C are controlled by D_L and D_C. Fig. 8 shows the schematic of the dual-band transmitter with the RSN high frequency transmitter shaded. Here R_{tx} and X_{tx} are the resistance and reactance of the low frequency coils. In this circuit, Q_1 and Q_2 operate as one phase-shift half-bridge, and Q_3 and Q_4 operate as the other phase-shift half-bridge. The duty ratios of of the two half-bridges modulate M_C and M_L, and the phase difference between the two half-bridges modulates the power output of the LF transmitter.

Benefiting from the low pass filters at the output of the dc-dc converters and the input inductors of the Class-E inverters, the LF transmitter and the HF transmitter are well-decoupled from each other. θ_C and θ_L modulate the LF transmitter, but have no impact on M_C and M_L, and thus have no impact on the HF transmitter. Similarly, Φ_C and Φ_L modulate the HF transmitter, but have no impact on the LF transmitter. When D_C and D_L are adjusted to modulate M_C and M_L, θ_C and θ_L should be changed accordingly to maintain the power level of the LF transmitter. The two overlapped transmitter coils and the related resonant tanks are optimally tuned for 100 kHz and 13.56 MHz, respectively [2].

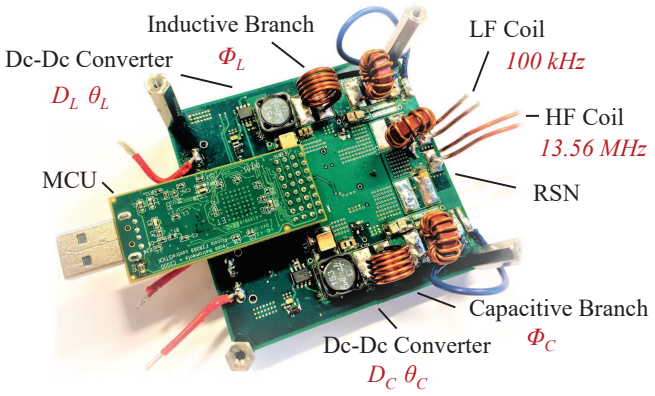

Fig. 10. The dual-band transmitter with an inductive branch, a capacitive branch, a micro-controller (MCU) and a RSN.

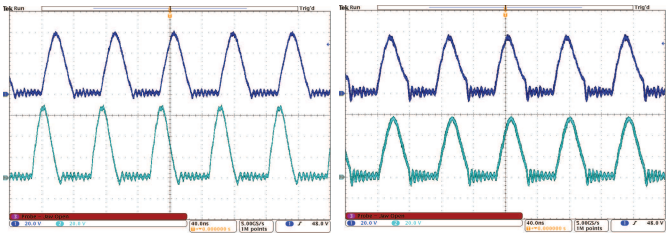

(a) (b)

Fig. 11. Measured drain-to-source voltage of the two HF switches: (a) ZVS with RSN operation, (b) non-ZVS without RSN operation. The load impedance Z_{tx} is $100.6 - 66.2j\Omega$, the delivered power is 10W. There is a 90 degree phase shift between the inductive branch and capacitive branch.

TABLE I
Passive Component Values of the Dual-Band Transmitter.

$L_{f,C}$ 200 nH	$L_{0,C}$ 870 nH	$C_{S,C}$ 260 pF	$C_{0,C}$ 160 pF	C_{RSN} 220 pF	C_1 100 uF	L_1 10 uH
$L_{f,L}$ 200 nH	$L_{0,L}$ 870 nH	$C_{S,L}$ 260 pF	$C_{0,L}$ 160 pF	L_{RSN} 620 nH	C_2 100 uF	L_2 10 uH

V. Experimental Verification

Fig. 9 shows a prototype DBMR WPT system comprises a 100 kHz transmitter, a 13.56 MHz transmitter, a 100 kHz receiver, and a 13.56 MHz receiver. The dual-band transmitter is shown in Fig. 10. The component values of the two converter channels are listed in Table I. The input inductors of the two Class-E inverters, $L_{f,C}$ and $L_{f,L}$, are designed to resonant with the shunt capacitors, $C_{S,C}$ and $C_{S,L}$, following the method described in [9]. The resonant frequency of the output tank of the two Class-E inverters, $L_{0,C}C_{0,C}$, $L_{0,L}C_{0,L}$, are 13.56 MHz. The two HF switches are GaN transistors (GS66504B). The output capacitance of the two HF switches (around 60 pF) are absorbed into the shunt capacitors $C_{S,C}$ and $C_{S,L}$. Fig. 11 shows the ZVS operation of the HF switches with $Z_{tx} = 100.6 - 66.2j\Omega$ and 10 W of delivered power.

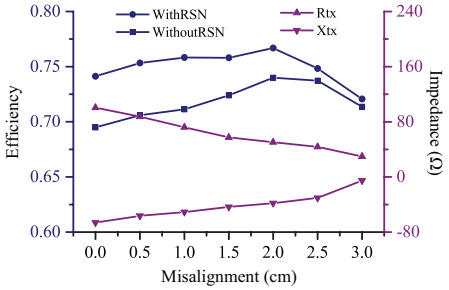

Fig. 12. Measured end-to-end efficiency of the DBMR WPT system and the input impedance of the HF coil as a function of the coil misalignment.

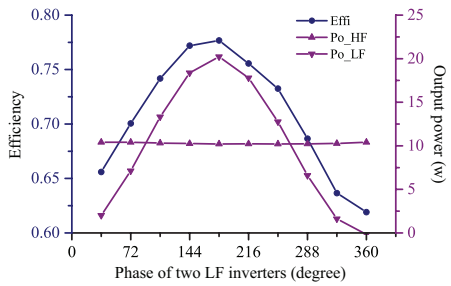

Fig. 13. Maintaining a constant Po_HF and modulating Po_LF when low frequency and high frequency systems are working simultaneously.

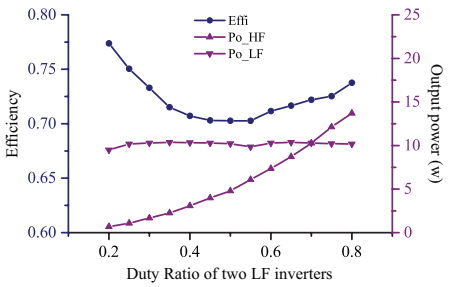

Fig. 14. Maintaining a constant Po_LF and modulating Po_HF when low frequency and high frequency systems are working simultaneously.

A 100 kHz receiver and a 13.56 MHz receiver are designed and tested to evaluate the end-to-end dc-dc performance. The 100 kHz receiver is a full-bridge diode-rectifier rectifier, and the 13.56 MHz receiver is a push-pull Class-E rectifier. Following a similar reconfiguable concept, one can merge the full-bridge diode-rectifier and the push-pull Class-E rectifier as a dual-band rectifier. The diameters of the HF coil and the LF coil are 10 cm and 20 cm, respectively. The distance between the transmitting coil and receiving coil is 2 cm. The maximum horizontal misalignment is 5 cm. Fig. 12 shows the measured end-to-end efficiency of the 13.56 MHz WPT system and the input impedance of the HF transmitting coil as a function of the coil misalignment. As expected, the input impedance of the transmitting coil, R_{tx} and X_{tx}, decreases as the misalignment increases. The X_{tx} reaches the peak when the two coils are close to each other. We also measured the efficiencies of this prototype with and without using the RSN. As shown in Fig. 12, the system with the RSN achieves higher efficiency than the system without the RSN across the entire misalignment range. When the load reactance is very high, the RSN increases the efficiency from 70% to 75%.

Fig. 13 and Fig. 14 show the experimental results with the LF and HF systems working together. The prototype DBMR WPT system can independently controlling the output power of the LF transmitter and HF transmitter. The output power of the LF transmitter is controlled by the duty ratio D_L, D_C, and the phase shift θ_L and θ_C. The output power of the HF transmitter is controlled by the relative voltage ratio M_L, M_C, and the phase shift Φ_L and Φ_C. The operation of the two frequency bands are independent from each other with negligible cross-coupling effects. As shown in Fig. 13, by keeping D_L, D_C, Φ_L, Φ_C as constants, and modulating the phase difference between θ_L and θ_C form 0 to 2π, the power transferred at 100 kHz (Po_LF) can be modulated between 0 W to 20 W, and the power transferred at 13.56 MHz (Po_HF) can be kept constant at 10 W. Similarly, as shown in Fig. 14, one can keep the power transferred at 13.56 MHz constant at 10 W, and modulates the power transferred at 100 kHz from 0 W to 15 W by changing the duty ratio of the LF inverters. The measured efficiencies of the HF and LF transmitters working together are shown in Fig. 13 and Fig. 14, respectively. When delivering 10 W of power at 13.56 MHz, and delivering 20 W of power at 100 kHz, the system reaches a maximum end-to-end efficiency of 77.7%.

VI. Conclusions

A dual-band WPT architecture targeting multi-receiver applications with significant coil misalignment and load variation is presented in this paper. This architecture is developed based on a novel reactance steering network (RSN) that can precisely compensate an arbitrary load reactance by dynamically steering the reactive power between a two inverter branches. The RSN technique is applicable to a variety of high frequency power conversion applications. We developed the theory of RSN and presented a design method that can cover an arbitrary reactance variation range. This approach is experimentally verified by a 50 W dual-band WPT system that can efficiently and independently power multiple 100 kHz and 13.56 MHz receivers with significant coil misalignment and load variation.

References

[1] G. Buja, M. Bertoluzzo and K. N. Mude, "Design and Experimentation of WPT Charger for Electric City Car," *IEEE Transactions on Industrial Electronics*, vol. 62, no. 12, pp. 7436-7447, Dec. 2015.

[2] B. H. Choi, V. X. Thai, E. S. Lee, J. H. Kim and C. T. Rim, "Dipole-Coil-Based Wide-Range Inductive Power Transfer Systems for Wireless Sensors," *IEEE Transactions on Industrial Electronics*, vol. 63, no. 5, pp. 3158-3167, May 2016.

[3] T. Campi, S. Cruciani, F. Palandrani, V. De Santis, A. Hirata and M. Feliziani, "Wireless Power Transfer Charging System for AIMDs and Pacemakers," *IEEE Transactions on Microwave Theory and Techniques*, vol. 64, no. 2, pp. 633-642, Feb. 2016.

[4] P. Raval, D. Kacprzak and A. P. Hu, "Multiphase Inductive Power Transfer Box Based on a Rotating Magnetic Field," *IEEE Transactions on Industrial Electronics*, vol. 62, no. 2, pp. 795-802, Feb. 2015.

[5] N. O. Sokal and A. D. Sokal, "Class E-A new class of high-efficiency tuned single-ended switching power amplifiers," *IEEE Journal of Solid-State Circuits*, vol. 10, no. 3, pp. 168-176, Jun 1975.

[6] Y. Han, O. Leitermann, D.A. Jackson, J.M. Rivas, and D.J. Perreault, "Resistance compression networks for radio-frequency power conversion," *IEEE Transactions on Power Electronics*, Vol. 22, No.1, pp. 41-53, Jan. 2007.

[7] S. Sinha, A. Kumar and K. K. Afridi, "Active variable reactance rectifier: A new approach to compensating for coupling variations in wireless power transfer systems," *IEEE Workshop on Control and Modeling for Power Electronics (COMPEL)*, Stanford, CA, 2017, pp. 1-8.

[8] D. J. Perreault, "A new power combining and outphasing modulation system for high-efficiency power amplification," *IEEE Transactions on Circuits and Systems I: Regular Papers*, vol. 58, no. 8, pp. 17131726, Aug 2011.

[9] L. Roslaniec, A. S. Jurkov, A. A. Bastami, and D. J. Perreault, "Design of single-switch inverters for variable resistance/load modulation operation," *IEEE Transactions on Power Electronics*, vol. 30, no. 6, pp. 32003214, June 2015.

[10] S. Liu, M. Liu, S. Han, X. Zhu, and C. Ma, "Tunable Class E^2 dc-dc converter with high efficiency and stable output power for 6.78 MHz wireless power transfer," *IEEE Transactions on Power Electronics*, vol. 33, no. 8, pp. 6877-6886, Aug. 2018.